Novel Amphiphilic Dextran Copolymers Nanoparticles for Delivery of Doxorubicin

Hongxia Gao,[1,2] Mingjun Li,[2] Yan Wu[1]

[1]*National Center for Nanoscience and Technology, Laboratory of Nanobiomedicine and Nanosafety, Division of Nanomedicine and Nanobiology, Beijing, China, No.11 Beiyitiao, Zhongguancun Beijing 100190, China*
[2]*The First Affiliated Hospital of Jiamusi University, Jiamusi 154002, China*

Received 26 April 2010; accepted 27 September 2010
DOI 10.1002/app.33459
Published online 10 December 2010 in Wiley Online Library (wileyonlinelibrary.com).

ABSTRACT: In this work, a novel biodegradable amphiphilic copolymer based on dextran and 1,2-dipalmitoyl-sn-glycero-3-phosphoethanolamine (DPPE) was successfully prepared. The amphiphilic copolymer may self-assemble into polymeric micelles in an aqueous solution. Fluorescence spectroscopy, dynamic light scattering (DLS), and a transmission electron microscope (TEM) method confirmed the formation of copolymeric micelles. To estimate the feasibility as novel drug carriers, doxorubicin (DOX) was incorporated into polymeric nanoparticles. The DOX-loaded nanoparticles exhibited greater antitumor effect than free DOX for HeLa celles, suggesting that the dextran/DPPE nanoparticles have great potential as a tumor targeting drug carrier. © 2010 Wiley Periodicals, Inc. J Appl Polym Sci 120: 2448–2458, 2011

Key words: dextran; 1,2-dipalmitoyl-sn-glycero-3-phosp hoethanolamine; copolymeric nanoparticles; doxorubicin; drug delivery

INTRODUCTION

The unique physicochemical properties of amphiphilic polymers have attracted great interest because of their applications in many fields, which are related to their self-assembly into micellar systems. Current and potential applications of amphiphilic polymers include stabilizers, dispersants, emulsifiers, wetting agents, and nanoreservoirs.[1,2] In biomedical fields, amphiphilic polymers have been drawing significant attention as promising carriers in drug delivery and matrices in tissue engineering.[3–5] The aims of utilizing the polymeric micelles in drug delivery are to improve the solubility of water insoluble drugs, to stabilize and protect drugs which are sensitive to the surrounding environment, to reduce the nonspecific uptake by the reticuloendothelial system, to prolong the circulation time in the blood, and to achieve the targeting delivery. The most widely studied amphiphilic polymers for drug delivery include diblock copolymers and triblock copolymers. However, the conventional micelle drug delivery systems based on the linear amphiphilic copolymers suffer from low encapsulation efficiency and fast initial release rate, which limit their applications in drug delivery.[6,7] Recently, it has been shown that amphiphilic copolymers with nonlinear structure exhibited improved property as drug carriers.[8] In this study, we designed and synthesized a novel amphiphilic copolymer which contain hydrophobic 1,2-dipalmitoyl-sn-glycero-3-phosphoethanolamine (DPPE) moiety and a hydrophilic dextran chain. The hydrophilic part of this copolymer is dextran, which is commonly used in biomedical fields as drug carrier. The hydrophobic part is composed of DPPE moiety.[9] DPPE was chosen in our molecular design because of its biological origin, which may lead to better biocompatibility for polymer incorporated with DPPE moiety. As has been known, in aqueous media, certain polyethylene glycol/phosphatidylethanolamine (PEG-PE) conjugates form very stable micelles. The PEG-based corona makes these micelles long circulating, whereas the lipid hydrophobic core may be used as a cargo space for poorly soluble compounds, including many anticancer drugs.[10–12] The characteristic size, stability, and the longevity in the systemic circulation make PEG-PE micelles a promising carrier for the delivery of drugs to the ill site via the enhanced permeability and retention (EPR) effect.[13–16] However, the PEG-PE copolymers are expensive and one drawback of PEG-based copolymers is the absence of reactive groups at their molecular chains, which limits further modification or

Correspondence to: M. Li (xjl1362@sina.com) or Y. Wu (wuyan66@eyou.com).

Contract grant sponsor: Major Program for Fundamental Research of the Chinese Academy of Sciences; contract grant number: KJCX2-YW-M02.

Contract grant sponsor: State Key Development Program for Basic Research of China (973); contract grant numbers: 2009CB930200, 2010 CB934004.

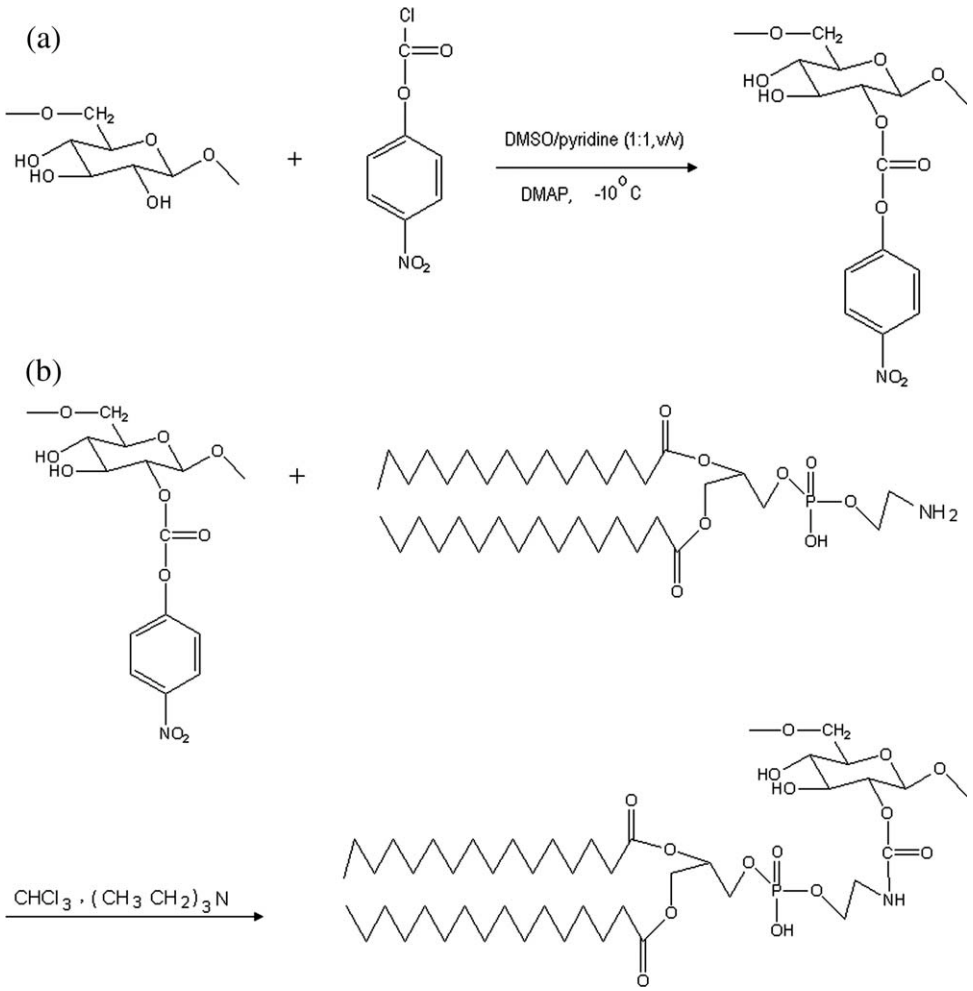

Scheme 1 Synthetic route of the copolymer dextran/DPPE: (a) synthetic route of the activation of dextran and (b) dextran/DPPE.

ligand coupling. In contrast, naturally occurring polysaccharides with good hydrophilicity, biocompatibility, and biodegradability seem to be attractive alternatives to PEG hydrophilic segments for designing amphiphilic copolymers.

In this study, we chemically conjugated biocompatible and hydrophobic DPPE chains onto the backbone of dextran by the activation of dextran using 4-nitrophenyl chloroformate and then the activated dextran/DPPE copolymer was prepared. Finally, activated dextran/DPPE copolymer was added to Tris buffer (pH 8.5) to prepare dextran/DPPE copolymer. The physical characteristics of dextran/DPPE self-assembled nanoparticles such as size, morphology, and critical aggregation behavior were studied. For practical applicability, anti tumor drug doxorubicin (DOX) was physically encapsulated into dextran/DPPE micelles. DOX-loaded dextran/DPPE nanoparticles were characterized, and the antitumor effect of the drug-loaded dextran/DPPE micelle nanoparticles was evaluated *in vitro*.

EXPERIMENTAL

Chemicals and materials

The 1,2-dipalmitoyl-sn-glycero-3-phosphoethanolamine (DPPE), dextran (6000 Da), 4-nitrophenyl chloroformate, 4-dimethylaminopyridine (DMAP), triethylamine (TEA), CL-4B Sepharose, and doxorubicin were purchased from Sigma-Aldrich and used without further purification. Dulbecco's modified eagle medium (DMEM) and dimethyl sulfoxide (DMSO) were obtained from GIBCO Invitrogen Corp. HeLa cells were kindly supplied by the Medical Department of First Affiliated Hospital of Jiamusi University in China and were chosen to investigate the biocompatibility in this article. All other reagents and solvents were of analytical grade.

Synthesis of dextran-DPPE

The activation of dextran (dextran-pNP) was performed as follows [Scheme 1(a)]: 2 g of dextran and

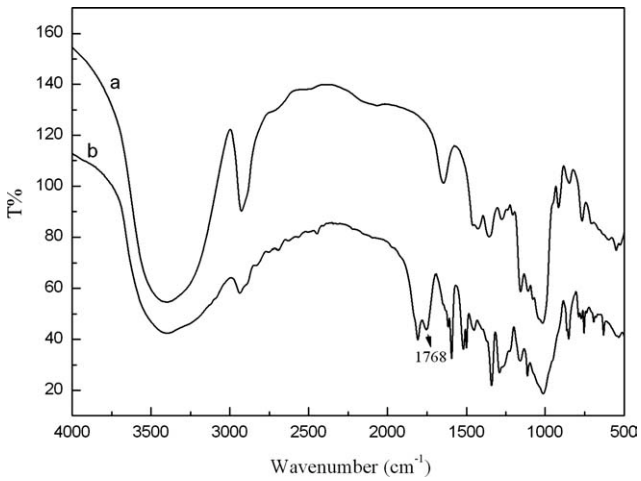

Figure 1 FT-IR spectra of dextran (a) and dextran-pNP (b).

50 mg of DMAP were dissolved in DMSO pyridine solution (1 : 1, v/v) by stirring and then 4-nitrophenyl chloroformate (5 g) was added to the solution and the both were allowed to react at -10°C by stirring. After 8 h, the reacted solution was added to ethanol and the precipitate collected and extensively washed off with ethanol.

The dextran-pNP/DPPE was synthesized as follows. A mixture of dextran-pNP and DPPE (contain 0.5 mol triethylamine, in the molar ratio of 1 : 3 to 1 : 15 dextran-pNP/DPPE) was suspended in 20 mL of chloroform with magnetic stirring at room under argon. After being stirred continuously for 12 h, the organic solvents were removed using a rotary evaporator. The dextran-pNP/DPPE was purified using RP-HPLC preparative column with methanol/0.01*M* HCl (70/30, v/v) as the mobile phase, which was removed by the vacuum evaporator. The dextran-pNP/DPPE was stored as a powder at −20°C.

To prepare dextran/DPPE copolymer [Fig. 1(b)] and remove the *p*-nitrophenyl carbonate group, the above dextran-pNP/DPPE was added to Tris buffer (pH 8.5), then mixed and incubated overnight at 4°C under an argon atmosphere. The dextran/DPPE copolymer was purified through the dialysis against distilled water at 4°C using a dialysis bag (MWCO of 3500 Da) for 24 h, after which samples were freeze-dried and stored as a powder at −20°C. The synthesized dextran/DPPE copolymer was analyzed by NMR spectra.

Characterization of dextran/DPPE copolymer

For FT-IR, the samples were then mixed with KBr and pressed to a plate for measurement. The scanning range was from 4000 to 500 cm^{-1}.

The nuclear magnetic resonance (^1H NMR, ^{13}C NMR, ^{31}P NMR) was recorded on a (Bruker AVANCE 400) NMR spectrometer. During the measurement, dextran was dissolved in DMSO-*d*6 and dextran/DPPE copolymers were dissolved in $CDCl_3$.

The molecular weight and molecular weight distribution of the copolymer were determined using gel permeation chromatography (GPC) equipped on a Waters 2410 GPC apparatus (USA). The eluent phase was THF and the molecular weights were calibrated with polystyrene standards.

The thermal stability of dextran/DPPE samples was measured by TGA (Perkin–Elmer, America). The temperature range was 25–900°C under nitrogen flow and the heating rate was 20°C min^{-1}.

Preparation of dextran/DPPE micelles

To formulate dextran/DPPE self-assembled micelle, dextran/DPPE copolymer (50 mg) was dissolved in 5 mL of DMSO and then the solution was dialyzed against deionized water for 1 day using a dialysis membrane (MWCO of 3500 Da).

Preparation of DOX-loaded dextran/DPPE nanoparticles

DOX-loaded dextran/DPPE nanoparticles were prepared by dissolving dextran/DPPE (50 mg) and DOX (10 mg) in 5 mL of DMSO, and mixed with an equal molar amount of triethylamine (TEA) to DOX for 4 h. The solution was then dialyzed against deionized water for 12 h using a dialysis membrane (MWCO of 3500 Da). The resulting aqueous solution was either lyophilized for further experiments or analyzed directly to determine the loading amount and efficiency. To evaluate the loading amount of DOX within dextran/DPPE nanoparticles, the above solution (100 μL) was mixed with DMSO (1.9 mL) to extract encapsulated DOX, and absorbance value at 485 nm was measured using a UV spectrophotometer [Perkin–Elmer Lambda850 (USA)]. DOX unloaded dextran/DPPE nanoparticles were used as a blank. The nanoparticles yield, drug-loading content, and drug entrapment efficiency were presented by eqs. (1)–(3), respectively:

$$\text{Nanoparticles yield}(\%) = \text{weight of nanoparticles}/\text{weight of polymer and drug feed initially} \times 100 \quad (1)$$

$$\text{Drug-loading content}(\%) = \text{weight of drug in}/\text{weight of nanoparticles} \times 100 \quad (2)$$

$$\text{Entrapment efficiency}(\%) = \text{weight of drug in nanoparticles}/\text{weight of drug feed initially} \times 100 \quad (3)$$

Each sample was assayed in triplicate.

Characterization of dextran/DPPE copolymer nanoparticles

Steady-state fluorescence spectra was recorded on a spectrofluorophotometer (FL-920 England) in that a solution of copolymers containing 6×10^{-7} *M* of pyrene was placed in a square cell and the fluorescence spectrum obtained with a fluorometer. The concentration of the sample solution varied from 1.0×10^{-4} to 0.5 mg/mL and the excitation wavelength (λex) was 336 nm.

The size and size distribution of the nanoparticles were measured using a Nano series ZEN 3600 (Malvern Instruments, England). All size measurements were done with a wavelength of 532 nm at 25°C with an angle detection of 90°.

The morphology of the micelles was performed using a transmission electron microscope (TEM, Hitachi, H-600). Before visualization, a droplet of nanoparticle suspension containing 2% w/w phosphotungstic acid was placed on copper grid and dried.

The morphology of the DOX-loaded dextran/DPPE nanoparticles was performed using a environmental scanning electron microscopy (ESEM, Quauta 200FEG, FEI) was used to observe the morphology of the nanoparticles. A drop of nanoparticle solution was deposited onto a silicon chip and air-dried before ESEM observation.

In vitro drug release of DOX from polymer nanoparticles

Freeze-dried nanoparticles samples (15 mg each) were resuspended in PBS or acetate buffered solutions and transferred into a dialysis tube (M_w cutoff: 3500 Da). The tubing was placed into 50 mL PBS or acetate buffered solutions. Release study was performed at 37°C in an incubator shaker. At selected time intervals, buffered solution outside the dialysis bag was removed for UV–vis analysis and replaced with fresh buffer solution. DOX concentration was calculated based on the absorbance intensity at 485 nm. Each experiment was repeated thrice and the result was the mean value of three samples.

In vitro cytotoxicity of blank nanoparticles

In vitro cytotoxicity was evaluated by MTT assay. A 6.0×10^3 HeLa cells were incubated in each well of a 96-well plate. After incubation for 24 h in an incubator (37°C, 5% CO_2), the cells were then incubated in a culture media containing nanoparticles at various concentrations at 37°C for 48 h. Then DMEM-containing micelle nanoparticles were replaced by fresh DMEM and 20 μL of MTT solution (5 mg mL^{-1}) was added. After incubation for 4 h, the MTT medium was removed from each well and 200 μL of DMSO was added, and then the mixture was stirred at room temperature. The optical density was measured at 570 nm with a Microplate Reader Model 550 (BIO-RAD, USA). The cell viable rate was calculated by the following equation: Cell viability (%) = $(A_{\text{treated}}/A_{\text{control}}) \times 100$, where A_{control} was obtained in the absence of micelle nanoparticles and A_{treated} was obtained in the presence of the micelle nanoparticles.[17]

In vitro antitumor effect of drug-loaded nanoparticles

Cytotoxicity was measured to evaluate the antitumor effect of the drug-loaded nanoparticles. HeLa cells were seeded into a 24-well plate (4.0×10^4 cells $well^{-1}$) containing 1 mL of DMEM. After incubation for 24 h (37°C, 5% CO_2), the culture medium was removed and DMEM containing DOX-loaded nanoparticles was added to each well. The cells were coincubated with DOX-loaded nanoparticles at 27°C for 4 h. Then the DMEM medium containing nanoparticles was replaced by 800 μL of fresh DMEM and the cells were further incubated at 37°C for a particular time period. Finally, 80 μL of MTT solution (5 mg mL^{-1}) was added to each well. After incubation for 4 h, the MTT medium was removed from each well and 600 μL of DMSO was added, and then the mixture was stirred at room temperature. Finally, the mixture was transferred into a 96-well plate. The optical density was measured as mentioned above.

RESULTS AND DISCUSSION

Synthesis and characterization of dextran/DPPE copolymer

A synthetic scheme of DPPE grafted dextran is shown in Scheme 1. First, dextran was activated. Several activation methods for polymer contained hydroxyl have been considered: tosylation,[18] esterification using 4-nitrophenyl chloroformate,[19,20] carbonyl diimidazole,[21] cyanogen halide,[22] and so on. In our work, 4-nitrophenyl chloroformate was selected for the activation of hydroxyl groups of dextran and synthesis dextran-pNP in copolymer [Scheme 1(a)]. The degree of carbonate substitution could be determined easily by UV analysis after alkaline hydrolysis. The degree of 4-nitrophenyl carbonate substitution was controlled by adjusting the amount of chloroformate added. The degree of substitution initially increased to reach a maximum value at 8 h (74%). Then, dextran-pNP-DPPE was synthesized by reaction of the dextran-pNP and DPPE under argon. Finally, Tris buffer (pH 8.5) was added, the pNP group was removed, and dextran/DPPE copolymer was prepared [Scheme 1(b)]. The M_w of the copolymers was controlled by the molar feed ratio of the DPPE to dextran-pNP. The different

TABLE I
Composition and Molecular Weight Distribution of Dextran/DPPE Copolymers[a]

Copolymer[b]	Molecualr weight of copolymer M_w (kDa)	M_n (kDa)	Polydispersity (M_w/M_n)
Dextran/DPPE (1 : 3)	16	13	1.23
Dextran/DPPE (1 : 6)	24	19	1.26
Dextran/DPPE (1 : 10)	30	23	1.30
Dextran/DPPE (1 : 15)	38	30	1.27

[a] Measured by GPC.

samples named 1/3 (feed ratio of dextran-pNP with DPPE), dextran-pNP/DPPE 1/6, dextran-pNP/DPPE 1/10, and dextran-pNP/DPPE 1/15, respectively, were synthesized. The final products of dextran/DPPE have good solubility in $CHCl_3$, DMSO andtetrahydrofuran (THF). The molecular weights and polydispersity indexes of the dextran/DPPE copolymers were shown in Table I. The amount of DPPE introduced to dextran-pNP increase with the molar ratio of DPPE to dextran-pNP. This indicated that the higher the content of DPPE, the higher the opportunity for the DPPE to react with dextran-pNP reactive centers.

Figure 1(b) showed the absorption peak at 1768 cm^{-1} was attributed to 4-nitrophenyl carbonates.[23]

Figure 2(b) showed the ^1H NMR spectrum of dextran/DPPE copolymer. Compared with dextran[24] [Fig. 2(a)], as seen in Figure 2(b), the signals at $\sim$ 0.9 ppm resulted from the terminal methyl proton of the DPPE moiety. The signals at $\sim$ 1.2–1.6 ppm were attributed to the methenyl protons of the DPPE moiety. All other absorption peaks were attributed to the protons of the DPPE moiety.[25] Compared with dextran [Fig. 2(c)], the ^{13}C NMR spectra of the dextran/DPPE copolymer [Fig. 2(d)] showed that the peak at $\sim$ 14 ppm was attributed to the terminal $-CH_3$ group carbon peak of the DPPE moiety. The

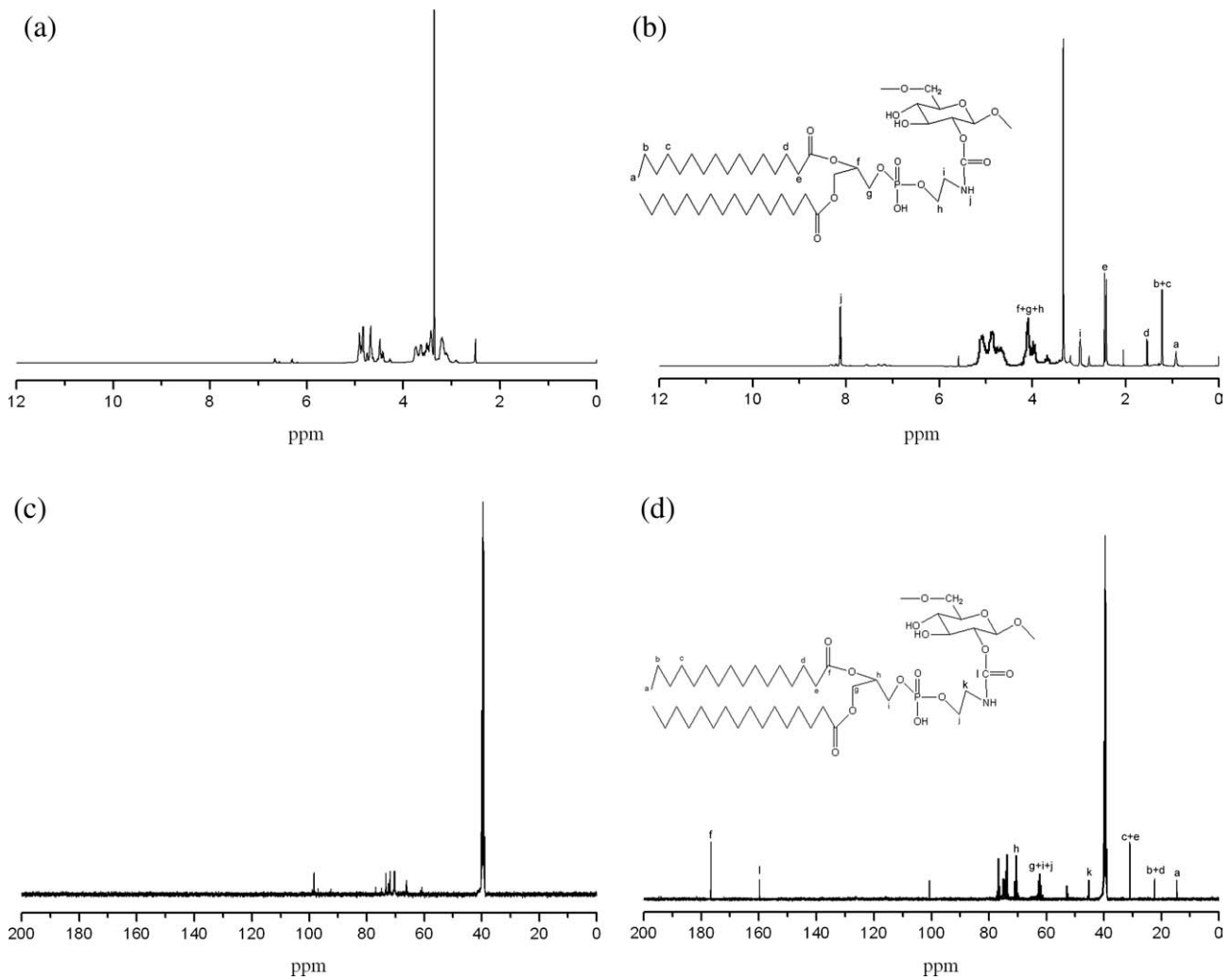

Figure 2 ^1H NMR spectrum of the dextran (a), dextran/DPPE (1 : 3) (b), and ^{13}C NMR spectrum of the dextran (c) and dextran/DPPE (1 : 3) (d).

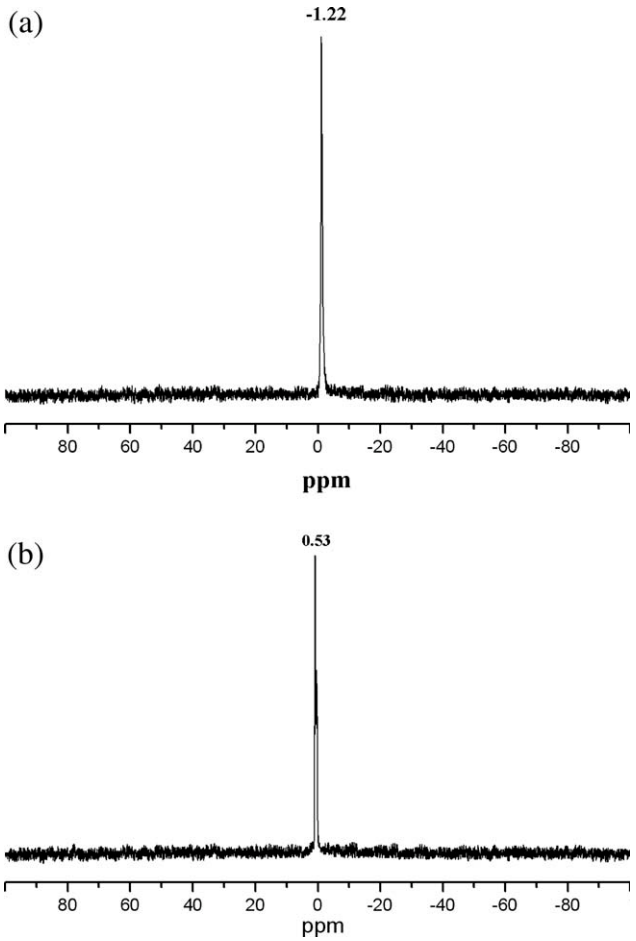

Figure 3 ^{31}P NMR spectrum of DPPE (a) and dextran/DPPE (1 : 3) (b).

signals at ~ 22 and 31 ppm were assigned to —CH_2 group carbon peak of the DPPE moiety. The signals at ~ 160 and 175 ppm were assigned to —COO group carbon peak of the DPPE moiety. All above these results evidenced that the copolymer contained DPPE side chains.

Furthermore, the typical ^{31}P NMR spectra of DPPE and dextran/DPPE copolymer is recorded and shown in Figure 3(a,b). Compared with DPPE [Fig. 3(a)] (−1.22 ppm), the ^{31}P NMR spectra of the dextran/DPPE copolymer [Fig. 3(b)] shows that the peak at 0.53 ppm is generally expected for ^{31}P functionalities.[26,27] The ^{31}P NMR spectra confirmed that phosphate groups are chemically bonded to the material. All these results evidenced that the copolymer contained DPPE side chains.

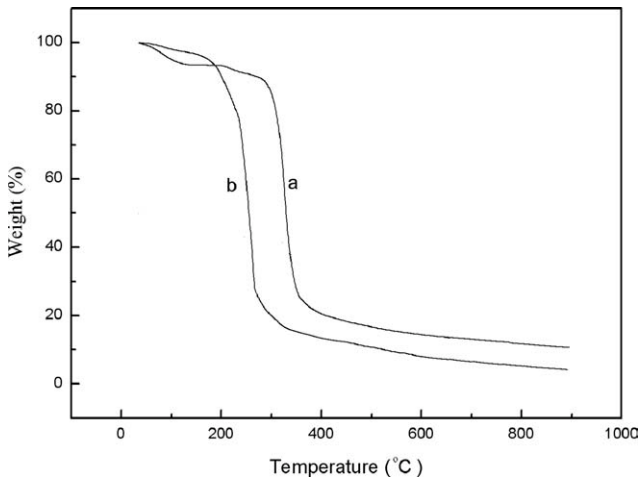

Figure 4 TGA graphs of dextran (a) and dextran/DPPE (1 : 10)(b).

TG curves of dextran and dextran-DPPE copolymer were shown in Figure 4(a,b). It could be seen that all of the copolymer samples exhibited a weight loss during the heating process. Compared with dextran [Fig. 4(a)], dextran-DPPE copolymer [Fig. 4(b)] has lower thermal degradation temperatures. A fast process of weight loss appears in the TG curves response for the copolymer in thermal degradation ranges. The thermo decomposed rate increased with increase of the rate of DPPE in the copolymers. These results indicated that the thermal stability of the copolymer was decreased with increase of DPPE chains.

Characterization of dextran/DPPE polymeric micelles and DOX-loaded dextran/DPPE polymeric micelle nanoparticles

Self-assembled dextran/DPPE micelles were prepared using a dialysis method as previously described. In

TABLE II
Effect of Different Composition of Copolymer on the Properties of Polymeric Nanoparticles and DOX-Loaded Polymeric Nanoparticles[a]

Sample	Copolymer	Mean diameter (nm)	Polydispersity	CMC × 10^3 (mg mL^{-1})
1	Dextran/DPPE (1 : 3)	51 ± 1.4	0.093–0.111	5.24
2	Dextran/DPPE (1 : 6)	72 ± 2.6	0.106–0.120	3.49
3	Dextran/DPPE (1 : 10)	90 ± 6.5	0.119–0.127	1.92
4	Dextran/DPPE (1 : 15)	110 ± 2.8	0.103–0.124	1.75
DOXNP3	Dextran/DPPE (1 : 3)	72 ± 4.7	0.115–0.126	4.77
DOXNP6	Dextran/DPPE (1 : 6)	94 ± 4.1	0.114–0.131	2.96
DOXNP10	Dextran/DPPE (1 : 10)	121 ± 5.3	0.130–0.145	1.83
DOXNP15	Dextran/DPPE (1 : 15)	133 ± 6.8	0.129–0.142	1.70

[a] DOX content 10% (w/w).

aqueous solution, hydrophobic interactions between grafted DPPE chains induced to form self-assembled nanostructures. It was likely that grafted hydrophobic DPPE chains were clustered in the micelle core, while the hydrophilic dextran backbone would be located on the shell layer. The average diameters of dextran/DPPE nanoparticles with different formulations and grafting percents are listed in Table II. The size of dextran/DPPE nanoparticles ranged from 51 to 110 nm. It appears that individual nanoparticles were composed of core/shell micelles self-assembled from hydrophobic DPPE cores and hydrophilic dextran shell layer. It is apparent that the grafting percent and molecular weight of grafted DPPE chains mainly affected the diameter of dextran nanoparticles. This was probably due to the effect of hydrophobic strength in the core packing on the size of micelles.

To further investigate the micellar formation of dextran/DPPE in aqueous solution, the critical micellar concentration (CMC) was measured using pyrene as a hydrophobic fluorescence probe. In studying the formation of micelle from hydrophobically-modified copolymer in aqueous solution, pyrene is generally used as a molecular probe and the variation in the ratio of intensity of first (372 nm) to third (383 nm) vibronic peaks I_{372}/I_{383}, the so-called polarity parameter, is quite sensitive to the polarity of microenvironment where pyrene is located. The change of the intensity ratio (I_{372}/I_{383}) was shown in Figure 5. For dextran/DPPE copolymer, at lower concentration, I_{372}/I_{383} values remain nearly unchanged. Further increasing concentration, the intensity ratio start to decrease, implying the onset of micelle from dextran/DPPE copolymer. The critical micelle concentration (cmc) was determined by the interception of two straight lines. From the CMC values (Table II), it was considered that the number of grafted DPPE chains onto the dextran backbone clearly affected the self-assembly behavior of dextran/DPPE. With increasing the grafting percent of DPPE, CMC values decreased, suggesting that more stable and compact dextran/DPPE nanoparticles were produced. Figure 5(c) showed the TEM image of polymeric micelles. It could be confirmed that polymeric micelles were regular spherical in shape.

The size and size distribution of copolymer nanoparticles (or DOX-loaded copolymer nanoparticles (DOXNP3, DOXNP6, DOXNP10, DOXNP15) were measured by DLS (Table II). The size of the plain copolymer nanoparticles was 51–110 nm in water. For these nanoparticles, the preparation conditions are same, so the chemical composition of the nanoparticles might be the main reason for difference of the mean diameter. According to the formation mechanism of nanoparticles, the mean diameter of

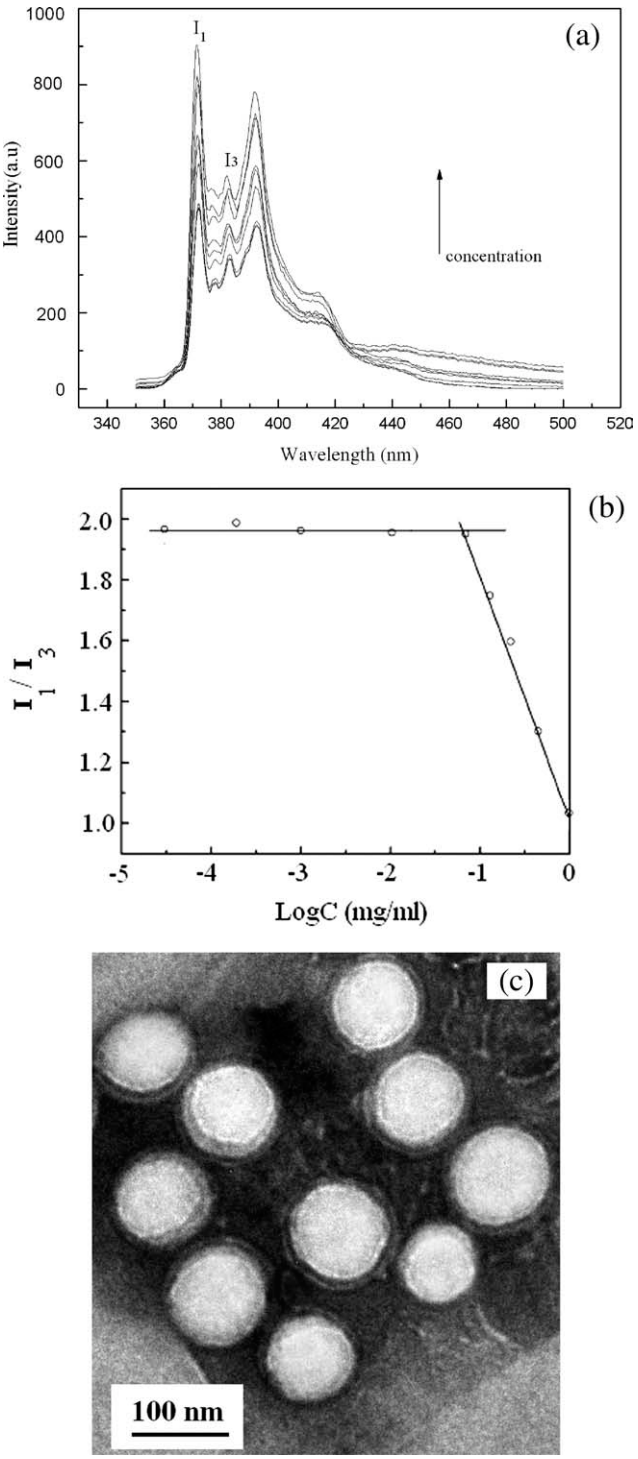

Figure 5 (a) Fluorescence emission spectra of pyrene in water in the presence of the dextran/DPPE copolymer at 20°C (copolymer concentration 0.0001, 0.003, 0.006, 0.01, 0.03, 0.06, 0.1, 0.25, 0.5 mg mL^{-1}); (b) Change of the intensity ratio (I_1/I_3) versus the concentration of the dextran/DPPE copolymer at 20°C; and (c) TEM of dextran/DPPE plain micelles (1 : 10).

nanoparticles was determined by the hydrophobic property of the core. The DLS data demonstrated that the nanoparticle size got larger as the DPPE

TABLE III
Drug Loading Efficiency, Drug Entrapment Efficiency, and Nanoparticles Yield of DOX-Loaded Polymeric Nanoparticles[a]

Sample	Copolymer	Entrapment efficiency (%)	Drug loading (%)	Nanoparticle yield (%)
1	Dextran/DPPE (1 : 3)	66.8 ± 1.2	7.6 ± 0.8	56.9 ± 2.1
2	Dextran/DPPE (1 : 6)	76.5 ± 2.5	8.5 ± 1.0	71.8 ± 2.6
3	Dextran/DPPE (1 : 10)	89.7 ± 3.4	11.7 ± 0.9	84.5 ± 1.5
4	Dextran/DPPE (1 : 15)	91.2 ± 1.1	12.4 ± 0.7	88.8 ± 2.2

[a] The mass of DOX used was 20% (w/w) in relation to polymer mass.

feed ratio increase suggesting the elongation of hydrophobic DPPE side chain facilitated the growth of the hydrophobic core of copolymer nanoparticles. These results indicated that the size of nanoparticles was dependent on the feed ratio of hydrophobic DPPE to dextran segment in the chain. The result was also in agreement with the characteristic of amphiphilic copolymer nanoparticles that the fewer the hydrophobic component, the smaller the nanoparticles. The DOX-loaded copolymer nanoparticles showed a larger size than the plain copolymer nanoparticles (Table II). It suggested that DOX was incorporated into the copolymer nanoparticles effectively. The detailed preparation condition, drug loading content, encapsulation efficiency, and the properties of the nanoparticles are summarized in Table III. As can be seen in Table III, the encapsulation efficiency (91.2%) of current system is much higher than the traditional systems based on the amphiphilic copolymers with linear structures. According to previous studies, the micelles self-assembled from the amphiphilic copolymers with nonlinear structures exhibit higher encapsulation efficiency and sustained drug release. In this study, the hydrophobic part of the amphiphilic copolymer is the DPPE moiety. The improved drug encapsulation property is attributed to the structure of the hydrophobic part of the copolymer. The drug-loading content in copolymer nanoparticles increased from 7.6 to 12.4% with the increase of the feed ratio of DPPE/dextran. This result could be explained that the DPPE moiety was favorable for interactions between DPPE and DOX. Therefore, the higher the DPPE content in copolymer, the more easily the drug was entrapped in copolymer nanoparticles. In addition, the interaction between of DPPE and DOX also contributed to an increased in EE%. It suggested that the elongation of hydrophobic DPPE side chain facilitated the compatibility of the hydrophobic segment of copolymer nanoparticles and antitumor drug DOX.

To characterize the morphology and size distribution of the DOX-loaded copolymer nanoparticles, ESEM and DLS measurement were carried out. Figure 6(a,b) showed the morphology and size distribution of DOX-loaded copolymer nanoparticles, respectively. It could be seen that drug-loaded nanoparticles are regularly spherical in shape and have a relatively narrow size distribution. Compared with the size determined by the Zetasizer (Table II), the particle size observed by ESEM is smaller. The variation in particle size measured by ESEM and Zetasizer is due to the fact that dynamic light scattering (DLS) measurement of the Zetasizer gives the hydrodynamic diameter rather than the actual diameter of the dried nanoparticles.

In vitro DOX release study

The *in vitro* release behaviors of DOX-loaded nanoparticles in two different buffered solutions (pH 7.4

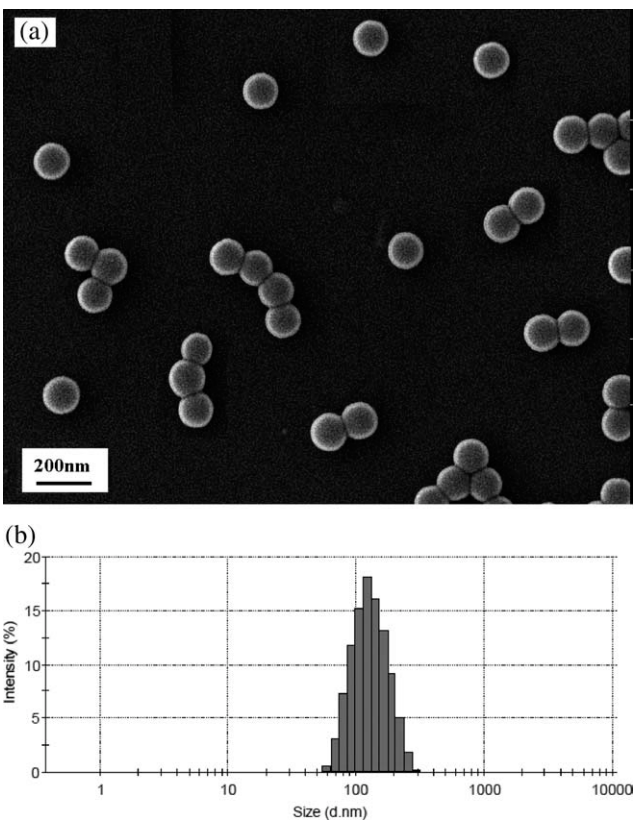

Figure 6 ESEM morphology of DOX-loaded dextran/DPPE (1 : 10) nanoparticles (a) and their size distribution determined by DLS (b) (1 : 10).

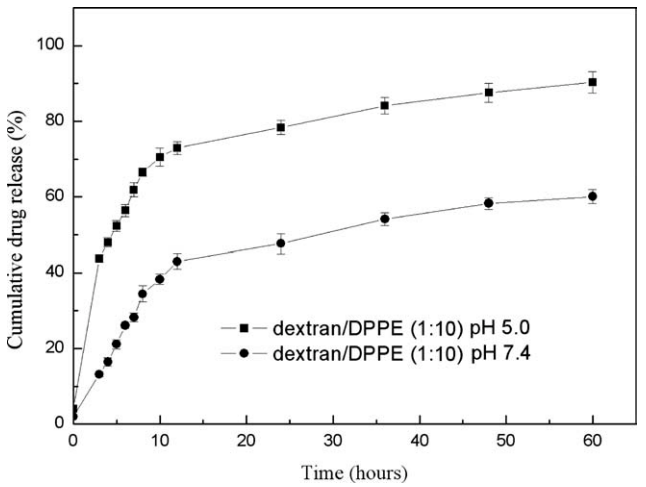

Figure 7 Release profiles of DOX from dextran/DPPE nanoparticles at neutral (pH 7.4) and acidic conditions (pH 5.0) at 37°C.

and 5.0) were studied and representatively shown in Figure 7. As shown in Figure 7, the release profiles show that DOX is released quickly from the nanoparticles in the initial stage and then the drug release could be sustained for more than 60 h. In comparison with the release at pH 5.0, DOX release from nanoparticles at pH 7.4 is much slower. The faster release of DOX in acidic conditions also was observed by Kataoka et al. with the DOX-loaded PEG-PBLA copolymer micelles,[28] and is likely due to the re-protonation of the amino group of DOX and faster degradation of micelle core at lower pH. This pH-dependent releasing behavior is of particular interest in achieving the tumor-targeted DOX delivery with micelle nanoparticles. It is expected that most DOX encapsulated in micelle nanoparticles will remain in the micelle cores for a considerable time period when the injected micelle nanoparticles stay in the plasma at normal physiological conditions (pH 7.4). However, a faster release will occur once the micelle nanoparticles reach the solid tumor site where pH value is lower than that in the normal tissue.[29] In addition, micellar nanoparticles are usually internalized inside the cells by endocytosis.[30] Therefore, a further accelerated release inside the endosome/lysosome of tumor cells may occur due to the decreased pH values.

Cytotoxicity of dextran/DPPE micelle nanoparticles and antitumor effect of drug-loaded nanoparticles

The effect of the concentration of dextran/DPPE micelle nanoparticles on the proliferation of HeLa cells was studied to investigate the cytotoxicity of the blank dextran/DPPE micelle nanoparticles and the data are shown in Figure 8(a). It is evident that the viabilities of HeLa cells in the presence of micelle nanoparticles are above 90% when the dextran/DPPE nanoparticle concentration is below 2.5 mg mL^{-1}, suggesting these micelle nanoparticles have good biocompatibility and low cytotoxicity to HeLa cells.

The antitumor effect of dextran/DPPE nanoparticles is examined by measuring the cytotoxicity of the DOX-loaded nanoparticles. As shown in Figure 8(b), when the concentration of DOX is low, the difference in antitumor effect between the free drug and different nanoparticles is not obvious. With the increasing concentration of DOX, the difference becomes distinct. Especially at a high DOX concentration of 42 μg mL^{-1}, the viabilities of HeLa cells incubated with free DOX, dextran/DPPE nanoparticles, and DOX-loaded dextran/DPPE (1 : 10) nanoparticles are 72.9% ± 1.4%, 95.8% ± 1.7%, and 22.1% ± 2.1%, respectively. The results revealed that DOX-loaded dextran/DPPE nanoparticles exhibited much higher cytotoxicity than free DOX. This enhanced cytotoxicity can

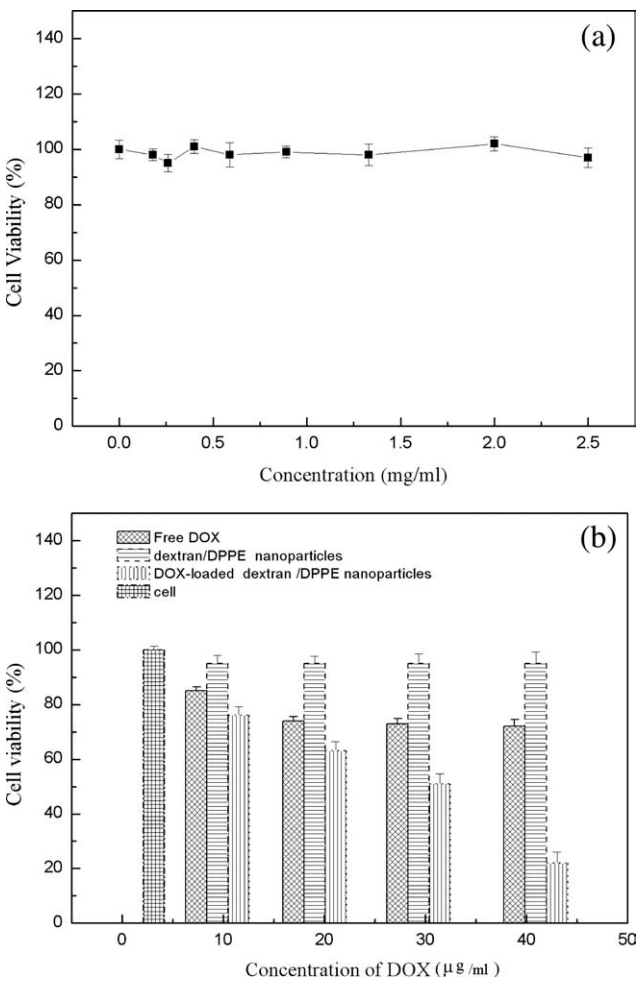

Figure 8 Cytotoxicity studies of the dextran/DPPE copolymer at different concentrations (a); viability of HeLa cells treated by free DOX and DOX-loaded dextran/DPPE nanoparticles with different free DOX concentrations (b).

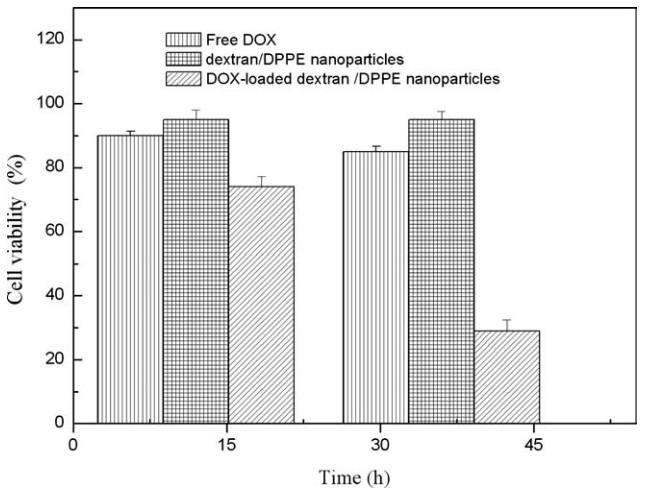

Figure 9 Viability of HeLa cells treated by free DOX and DOX-loaded nanoparticles. The cells were coincubated with free DOX and DOX-loaded nanoparticles with the free DOX concentration of 42 μg mL^{-1} for 4 h, and then the cells were further incubated in DMEM for 12 and 36 h, respectively.

also be explained by the enhanced cellular uptake of dextran/DPPE nanoparticles by endocytosis and the unique structure and properties of the DOX-containing dextran/DPPE nanoparticles may facilitate the entry of both DOX and dextran/DPPE. It should be noted that dextran/DPPE nanoparticles without DOX exhibited extremely low cytotoxicity (over 90% of cell survival) over the same polymer concentration range, confirming the enhanced cytotoxicity was not due to the effect of the dextran/DPPE nanoparticles.

Drug release inside the cells

To further investigate the drug release behavior of the dextran/DPPE nanoparticles inside the cells, the cell viability was determined after the cells were coincubated with drug-loaded micelle nanoparticles for 4 h and then incubated in drug-free DMEM for specific time intervals. As shown in Figure 9, after incubation in drug-free DMEM for 12 h, the viabilities of the HeLa cell treated with free DOX and DOX-loaded dextran/DPPE nanoparticles are 91 and 74%, respectively. When the incubation in drug-free DMEM is prolonged to 36 h, the cell viabilities of the HeLa cell treated with free DOX and DOX-loaded dextran/DPPE nanoparticles decreased to 85 and 29%, respectively. Clearly, the cell inhibition efficiency of drug-loaded DOX-loaded dextran/DPPE nanoparticles is higher due to the enhanced cellular uptake of dextran/DPPE nanoparticles and the unique structure and properties of the DOX-containing dextran/DPPE nanoparticles may facilitate the entry of both DOX and dextran/DPPE. Besides, the cell viability is also affected by the release rate of the drug from the nanoparticles inside the cells. Because of the sustained drug release from nanoparticles, the viabilities of the cells treated by nanoparticles could further decrease with increasing time.

CONCLUSIONS

Novel amphiphilic dextran/DPPE copolymers were synthesized. The synthesized dextran/DPPE copolymers self assembled in aqueous solution to form nano-sized micellar aggregates for delivery of DOX to cancer cells. When DOX was encapsulated within the nanoparticles, DOX-loaded dextran/DPPE nanoparticles showed increased extent of cellular uptake and enhanced cytotoxicity for HeLa cells. The present study demonstrated well that dextran/DPPE copolymer could be useful as biodegradable and biocompatible nano-structured carriers for intracellular delivery of anticancer drugs.

References

1. Allard, E.; Passirani, C.; Garcion, E.; Pigeon, P.; Vessières, A.; Jaouen, G.; Benoit, J. P. J Controlled Release 2008, 130, 146.
2. Oh, K. T.; Lee, E. S.; Kim, D.; Bae, Y. H. Int J Pharm 2008, 358, 177.
3. Vakil, R.; Kwon, G. S. Mol Pharm 2008, 5, 98.
4. Cha, E. J.; Kim, J. E.; Ahn, C. H. Eur J Pharm Sci 2009, 38, 341.
5. Na, H. S.; Lim, Y. K.; Jeong, Y. I.; Lee, H. S.; Lim, Y. J.; Kang, M. S.; Cho, C. S.; Hyun Chul Lee, H. C. Int J Pharm 2010, 383, 192.
6. Layre, A.; Couvreur, P.; Chacun, H.; Richard, J.; Passirani, C.; Requier, D. J Control Release 2006, 111, 271.
7. Savic, R.; Luo, L.; Eisenberg, A.; Maysinger, D. Science 2003, 300, 615.
8. Li, Y. Y.; Zhang, X. Z.; Kim, G. C.; Cheng, H.; Cheng, S. X.; Zhuo, R. X. Small 2006, 2, 917.
9. Lukyanov, A. N.; Gao, Z. G.; Mazzola, L.; Torchilin, V. P. Pharm Res 2002, 19, 1424.
10. Lukyanov, A. N.; Gao, Z. G.; Torchilin, V. P. J Controlled Release 2003, 91, 97.
11. Gao, Z.; Lukyanov, A. N.; Anurag Singhal, A.; Torchilin, V. P. Nano Lett 2002, 2, 979.
12. Lukyanov, A. N.; Elbayoumi, T. A.; Chakilam, A. R.; Torchilin, V. P. J Controlled Release 2004, 100, 135.
13. Wang, X.; Yang, L.; Chen, Z. G.; Shin, D. M. CA Cancer J Clin 2008, 58, 97.
14. Duncan, R. Nat Rev Cancer 2006, 6, 688.
15. Kataoka, K.; Harada, A.; Nagasaki, Y. Adv Drug Deliv Rev 2001, 47, 113.
16. Torchilin, V. P. J Control Release 2001, 73, 137.
17. Jeong, Y. I.; Cheon, J. B.; Kim, S. H.; Nah, J. W.; Lee, Y. M.; Sung, Y. K.; Akaike, T.; Cho, C. S. J Controlled Release 1998, 51, 169.
18. Nozaki, T.; Maeda, Y.; Ito, K.; Kitano, H. Macromolecules 1995, 28, 522.
19. Vandoorne, F.; Vercauteren, R.; Permentier, D.; Schacht, E. Mackromol Chem 1985, 186, 2455.
20. Vandoorne, F.; Bruneel, D.; Schacht, E. Bioact Compat Polym 1990, 5, 4.
21. Axén, R.; Ernback, S. Eur J Biochem 1971, 18, 351.

22. Laakso, T.; Stjärnkvist, P.; Sjöholm, I. J Pharm Sci 1987, 76, 134.
23. Chiu, H. C.; Hsiue, G. H.; Lee, Y. P.; Huang, L. W. J Biomater Sci Polym Edn 1999, 10, 591.
24. Shi, H. Y.; Zhang, L. M. Carbohydr Res 2006, 341, 2414.
25. Percot, A.; Briane, D.; Coudert, R.; Reynier, P.; Bouchemal, N.; Lièvre, N.; Hantz, E.; Salzmann, J. L.; Cao, A. Int J Pharm 2004, 278, 143.
26. Sabesan, S.; Neria, S. Carbohydr Res 1992, 223, 169.
27. Lebouc, F.; Dez, I.; Madec, P. J Polym 2005, 46, 319.
28. Kataoka, K.; Matsumoto, T.; Yokoyama, M.; Okano, T.; Sakurai, Y.; Fukushima, S.; Okamoto, K.; Kwon, G. S. J Controlled Release 2000, 64, 143.
29. Hoes, C. J. T.; Boon, P. J.; Kaspersen, F.; Feijen, J.;Makromol Chem Macromol Symp 1993, 70/71, 119.
30. Kakizawa, Y.; Kataoka, K. Adv Drug Deliv Rev 2002, 54, 203.